ChemComm

COMMUNICATION

View Article Online
View Journal | View Issue

Cite this: *Chem. Commun.*, 2014, **50**, 11576

Received 11th October 2013,
Accepted 13th August 2014

DOI: 10.1039/c3cc47840h

www.rsc.org/chemcomm

Counteracting the inhibitory effect of proteins towards lung surfactant substitutes: a fluorocarbon gas helps displace albumin at the air/water interface†

Phuc Nghia Nguyen,[a] Mariam Veschgini,[b] Motomu Tanaka,[b] Gilles Waton,[a] Thierry Vandamme[c] and Marie Pierre Krafft*[a]

Perfluorohexane gas lowers the kinetic barrier that opposes the displacement of albumin by dipalmitoylphosphatidylcholine at the air/water interface submitted to sinusoidal oscillations at frequencies in the range of those encountered in respiration.

A consequential roadblock in the treatment of acute respiratory distress syndrome (ARDS) is that serum proteins (*e.g.* albumins, globulins and fibrinogen) rapidly colonize the alveolar surface and hinder the access of this surface to phospholipids.[1–3] These proteins are involved through complex mechanisms in this high mortality condition, and their concentration in the alveolar fluids of ARDS patients correlates with the severity of the disease.[3] Most important is the hindering of the access of dipalmitoylphosphatidylcholine (DPPC) by albumin to the air/water interface. DPPC is indeed the main component of the native lung surfactant (LS) and of the therapeutic substitutes of the LS. This results in inactivation of such LS substitutes.[4,5] The blockage of the access to the interface exerted by albumin originates from a kinetic barrier, since DPPC has a lower equilibrium surface tension than the protein in water.[3] Strategies for facilitating the replacement of proteins by DPPC consist of lowering this kinetic barrier by increasing the concentration of the electrolytes (mono- or divalent ions that reduce the Debye length and screen the double-layer repulsion), or by promoting depletion interactions by hydrophilic polymers (such as poly(ethylene glycol) or hyaluronic acid).[3,4]

We have recently found that DPPC, which, according to all studies achieved under static conditions, does not adsorb significantly at an air/water interface when bovine serum albumin (BSA) is present[6] and, therefore, cannot exercise its interfacial tension lowering effect, does displace BSA from the interface and does lower the interfacial tension when the adsorbed film is submitted to prolonged sinusoidal oscillations.[7] The frequency of the oscillations for which BSA displacement is maximal lies within the range of those of human respiration under normal conditions. The oscillations were shown to induce a dilute-to-condensed phase transition in both DPPC films[8] and DPPC–BSA mixed films.[7] Under oscillations, total replacement of BSA by DPPC requires however ~11 h.[7] Acceleration of the protein replacement process is highly desirable, especially for the design, evaluation and practicability of LS substitutes. More generally, such an acceleration would facilitate the investigation of dynamic and transport properties in systems for which reaching equilibrium is quasi-forbidden due to extremely slow adsorption kinetics under standard experimental conditions and practical time-frames.

Our strategy was to control the self-assembly of phospholipids at the air/water interface using a fluorocarbon gas. We and others have indeed established that fluorocarbons and fluorocarbon emulsions can greatly facilitate DPPC re-spreading[9–13] and prevent the deleterious effect of BSA penetration in DPPC monolayers.[13] Fluorocarbons have been widely investigated for biomedical applications, including as intravascular oxygen carriers[14] and osmotic stabilizers for theranostic microbubbles.[15,16] Fluorocarbons are generally considered as biologically inert, in contrast to fluorinated surfactants that have recently raised concerns.[17] Fluorinated chains are both extremely hydrophobic and have a pronounced lipophobic effect as well. To the best of our knowledge, fluorocarbons have never been used to manipulate the properties of phospholipid films, in particular biointerfaces, in which there is a delicate interplay between phospholipids and proteins.

Here, we report on the kinetics of the competitive adsorption of DPPC and BSA at the interface between perfluorohexane (*F*-hexane)-saturated air and Hepes buffer. We show that, when prolonged sinusoidal oscillations are applied, *F*-hexane drastically accelerates the replacement of BSA by DPPC. This replacement becomes complete and irreversible.

The adsorption of DPPC and BSA has been studied in two distinct experimental configurations. In the first configuration, bubble profile analysis tensiometry was used at the interface of a millimetric

[a] *Systèmes Organisés Fluorés à Finalités Thérapeutiques (SOFFT), Institut Charles Sadron (ICS) CNRS, Université de Strasbourg (UPR 22), 23 rue du Loess, 67034 Strasbourg Cedex 2, France. E-mail: krafft@unistra.fr*
[b] *Physical Chemistry of Biosystems, Institute of Physical Chemistry, University of Heidelberg, Im Neuenheimer Feld 253, 69120 Heidelberg, Germany*
[c] *Laboratoire de Conception et Application de Molécules Bioactives (CNRS UMR 7199), Université de Strasbourg, 74 route du Rhin, 67401 Illkirch Cedex, France*

† Electronic supplementary information (ESI) available: Materials and experimental methods section and supporting data on BSA, DPPC and DPPC–BSA kinetic adsorption, DLS characterization of vesicles, and fluorescence micrographs of BSA interfacial films. See DOI: 10.1039/c3cc47840h

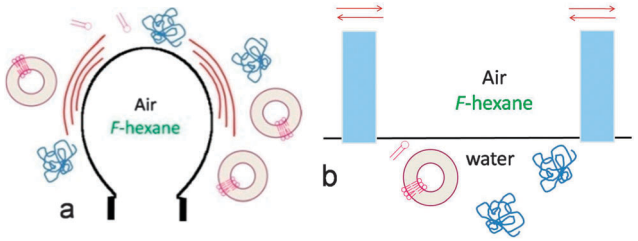

Scheme 1 Schematic representation of DPPC vesicles (red) and BSA molecules (blue) adsorbed from water (a) at the surface of an oscillating *F*-hexane-saturated air bubble in water and (b) at the planar air/water interface of a Langmuir trough with barriers impressing sinusoidal oscillations (not to scale).

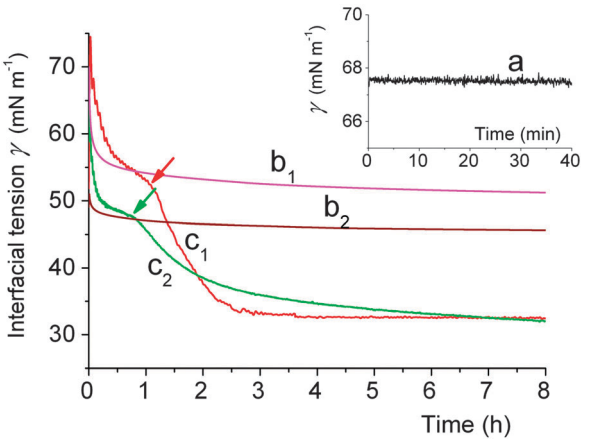

Fig. 1 Kinetics of adsorption (37 °C) at the surface of an air bubble of (a) *F*-hexane, (b) BSA (7.5×10^{-7} mol L^{-1}) and (c) DPPC (10^{-3} mol L^{-1}, provided as a dispersion of vesicles). In (b) and (c) the components are adsorbed at the surface of a bubble of air alone ($_1$) or a bubble of air saturated with *F*-hexane ($_2$). All the bubbles were submitted to oscillations (T 10 s, ΔA 15%) throughout the experiments. All the curves correspond to mean values obtained by treating the data (*i.e.* the fluctuations in interfacial tension associated with the oscillations) through a low-pass digital filter.

bubble of *F*-hexane-saturated air submitted to sinusoidal oscillations at 37 °C (Scheme 1a). The bubble was submitted to prolonged sinusoidal oscillations for a period T of 10 s (*i.e.* a frequency f of 0.1 Hz) and an amplitude ΔA of 15% of the bubble's surface area. The second configuration consists of dynamic surface pressure measurements within a Langmuir trough under the oscillating surface area. In the latter configuration, DPPC, BSA and DPPC–BSA mixtures were injected into the water subphase and sinusoidal oscillations (T 33 s, ΔA 15%) were applied to the adsorbed planar film *via* two oscillating barriers. In addition, these measurements were combined with epifluorescence microscopy at the air/water interface using DPPC and BSA labelled with a fluorescent probe, Texas Red. In both configurations, DPPC was provided in the form of vesicles (with a controlled size of 60–80 nm) dispersed in the Hepes buffer (pH 7.4).

The concentration of DPPC was 10^{-3} mol L^{-1} and that of BSA was 7.5×10^{-7} mol L^{-1}. In the case of competitive adsorption, the DPPC/BSA ratio was $1 \times 10^{-3} : 7.5 \times 10^{-7}$ mol L^{-1} (unless otherwise mentioned). These concentrations correspond to the ~10 : 1 (w/w) DPPC/BSA weight ratio typically found in the native lung surfactant.

A first important result is that *F*-hexane alone adsorbs rapidly at the air/water interface, as shown by an immediate reduction of the air/water interfacial tension by ~5 mN m^{-1} (from 71.7 to 67.6 mN m^{-1}; Fig. 1a, inset) for the bubble configuration.

Let us examine the behaviour of BSA when adsorbed alone at the interface submitted to oscillations, the air in the bubble being saturated, or not, with *F*-hexane (Fig. $1b_{1-2}$).

The BSA concentration investigated is well above the critical concentration at which BSA adsorption at the interface is no longer controlled by its diffusion through the solution, but is hindered by the interfacial energy barrier.[18,19] The rate of adsorption is determined by the ability of BSA molecules to rearrange in the interfacial film. Such rearrangements are accompanied by partial unfolding of the protein resulting in the formation of tails and loops, with the hydrophilic sequences stretched in water and the hydrophobic parts collapsed at the interface.[19] We describe the adsorption kinetics by the characteristic time t_1 for the transfer of BSA molecules from the buffer solution to the interface. This time was measured by fitting the experimental $\gamma = f(\text{time})$ curves using an exponential decay function (see ESI,† Fig. S1). Each experiment was repeated at least three times.

In the Hepes buffer (pH 7.4), the negatively charged BSA adsorbs weakly at the interface, leading to moderate lowering of the interfacial tension γ (to ~51 mN m^{-1}). The characteristic time t_1 was found to be ~0.4 h under oscillations. The presence of *F*-hexane slightly increases the adsorption kinetics of BSA (Fig. $1b_2$), which was characterized by a t_1 of ~0.3 h. The equilibrium interfacial tension γ_{eq} decreases by ~5 mN m^{-1}.

When DPPC is adsorbed alone at the air/water interface, the adsorption dynamics are characterized by a dilute-to-condensed state phase transition (Fig. $1c_{1-2}$). Two characteristic times are required for the description of the kinetics: t_1 for the adsorption of the DPPC molecules at the interface and t_2 for the transfer of DPPC molecules from the dilute phase to the condensed phase. We determined t_1 and t_2 by fitting the experimental $\gamma = f(\text{time})$ curves using an exponential decay function (see ESI,† Fig. S2).

When *F*-hexane is present in the bubble's gas phase, the t_1 of DPPC adsorption strongly decreases from 0.27 h to 0.09 h. A likely reason for this is that *F*-hexane contributes to breaking the hydrogen bond network between water molecules at the air/water interface that opposes adsorption of molecules in solution. This effect impacts DPPC more strongly than BSA, for which only a modest effect of the fluorocarbon was detected. As a consequence of the increased recruitment of DPPC molecules at the interface, the dilute-to-condensed transition intervenes faster (~0.7 h instead of ~1.1 h) and at a lower γ (~47.2 mN m^{-1} instead of ~51.6 mN m^{-1}) (Fig. $1c_{1-2}$, arrows). On the other hand, where the second regime is concerned, t_2 is increased by a factor of ~3 when *F*-hexane is present. This means that *F*-hexane retards the ordering of the DPPC molecules at the interface by remaining in contact with the DPPC chains. However, γ_{eq} eventually reaches essentially the same value (~32.5 mN m^{-1}), showing that the fluorocarbon is totally expelled from the interfacial film after 6–7 h.

The adsorption of BSA and DPPC as single components was also investigated at a planar air/water interface submitted to sinusoidal oscillations. For BSA, the adsorption profile was similar to that obtained in the bubble configuration (γ_{eq} = 54 mN m^{-1}; see ESI,† Fig. S3). For DPPC, a change in slope occurs at ~0.7 h and ~65 mN m^{-1}. This change may indicate a dilute-to-condensed transition, although less

pronounced than for the bubble experimental configuration, and γ reaches its minimal value after ~1.5 h. These characteristics are in good agreement with those observed in the bubble configuration, but for the DPPC γ_{eq} value, which is somewhat higher (~45 mN m^{-1}) than in the case of the bubble (~32.5 mN m^{-1}). This discrepancy might be due to the difference in size of the interfaces in the two configurations. Altogether, these results demonstrate that the adsorption profiles of BSA and DPPC (as single components) are comparable at a bubble interface and at a planar interface.

Let us now examine the competitive adsorption of DPPC *versus* BSA in Hepes using the bubble configuration. The adsorption kinetics of the two components at the surface of the bubble shows two distinct regimes (Fig. 2). In the absence of *F*-hexane, the competitive adsorption profile of the DPPC–BSA mixture (Fig. 2a) is at first superimposed to that of BSA when adsorbed alone (Fig. 2c); t_1 = 0.4 h in both cases. After ~9.8 h (see arrow), a second regime sets in, which is characterized by a sharper decrease of γ, reflecting the progressive adsorption of DPPC at the interface.

The dilute-to-condensed phase transition seen on the adsorption profile of DPPC when adsorbed alone (Fig. 1c$_1$) is also observed for the mixed DPPC–BSA system at essentially the same γ value, that is, ~48.8 mN m^{-1} (arrows). However, the presence of BSA strongly increases t_2 (from 0.7 to 11.2 h; ESI,† Fig. S4). After ~23 h, γ reaches its lowest value of ~32 mN m^{-1}, similar to that measured for pure DPPC. The latter means that the BSA molecules have been displaced from the interface and replaced by DPPC molecules. This behaviour is highly reproducible, provided the DPPC vesicles have a similar small size (here ~80 nm; ESI,† Fig. S5).

In the presence of *F*-hexane, the adsorption profile of the DPPC–BSA mixture is at first similar to that of BSA when adsorbed alone (t_1 = 0.28 h in both cases). However, the dilute-to-condensed transition occurs remarkably faster (~2.5 h *versus* 9.8 h; see arrows in Fig. 2) than in the absence of *F*-hexane and at a comparable γ value (45.6 *versus* 47.8 mN m^{-1}). Also significant is that the presence of *F*-hexane decreases t_2 by nearly one order of magnitude, from 11.2 h to 1.6 h. This means that, contrary to what was observed in the case of DPPC alone, the presence of *F*-hexane no longer hinders the organisation of the phospholipid in its condensed phase. The γ_{eq} eventually reaches a slightly higher value (~34 *vs.* 32 mN m^{-1}), meaning that some *F*-hexane molecules have remained trapped in the DPPC monolayer.

The kinetic data are compared in Table 1, which displays the characteristic times t_1 and t_2 of the adsorption profiles.

The competitive adsorption of DPPC and BSA at the planar air/water interface has also been monitored by fluorescence microscopy. In these experiments, BSA and DPPC were injected into the Langmuir trough sequentially. First, a mixture of BSA and 2 mol% BSA-Texas Red was injected in the Hepes subphase, followed by DPPC 1.5 h later. Fig. 3 shows the variation of γ as a function of time in the presence and absence of *F*-hexane. When the fluorocarbon gas is present, γ is seen to decrease immediately after the injection of DPPC and reaches a plateau value of ~45 mN m^{-1} after ~4 h. By contrast, when the fluorocarbon is absent, γ remains more or less constant for ~2 h, before slowly decreasing and finally plateauing at ~45 mN m^{-1} after 7 h.

Fluorescence microscopy was used to visualize the appearance of the condensed phase of DPPC. This was done by monitoring the competitive adsorption of DPPC and BSA supplemented by 2 mol% of BSA-Texas Red. In the presence of *F*-hexane, dark structures appear after ~2.3 h (*i.e.* 0.8 h after DPPC injection) (Fig. 4a$_1$). These darker structures were identified as domains of the condensed phase of DPPC, as they are not seen when BSA alone is adsorbed at the interface (see ESI,† Fig. S6). These condensed phase domains

Table 1 Characteristic times t_1 and t_2 for the adsorption of DPPC, BSA, and DPPC–BSA combinations on the surface of bubbles filled with air or with *F*-hexane-saturated air and submitted to oscillations (T 10 s, ΔA 15%)

t (h)	DPPC	BSA	DPPC–BSA	DPPC/ *F*-hexane	BSA/ *F*-hexane	DPPC/BSA/ *F*-hexane
t_1	0.27	0.39	0.90	0.09	0.28	0.28
t_2	0.66	—	11.2	1.37	—	1.57

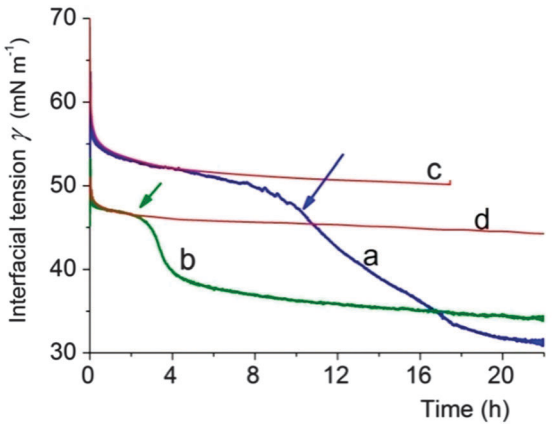

Fig. 2 Competitive adsorption kinetics (37 °C) of DPPC (1 × 10^{-3} mol L^{-1}) and BSA (7.5 × 10^{-7} mol L^{-1}) at the surface of (a) a bubble of air and (b) a bubble of air saturated with *F*-hexane. All the bubbles were submitted to oscillations (T 10 s, ΔA 15%) throughout the experiments. In red, for reference, the adsorption profiles of BSA (c) in the absence and (d) in the presence of *F*-hexane.

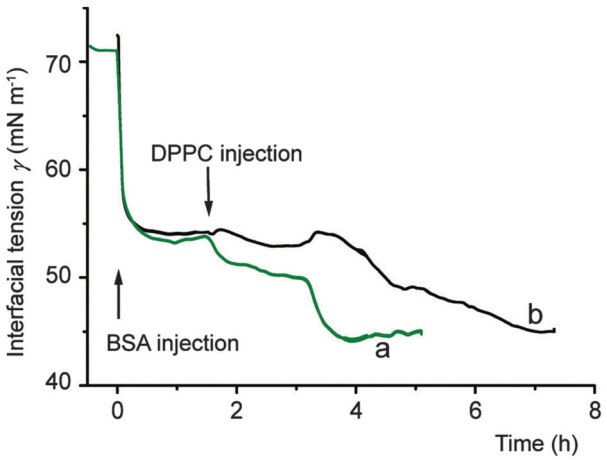

Fig. 3 Sequential adsorption kinetics (37 °C) of DPPC (3 × 10^{-3} mol L^{-1}) and BSA (7.5 × 10^{-7} mol L^{-1}) at the planar air/Hepes buffer interface in the presence of *F*-hexane (a) or in its absence (b). *F*-Hexane was allowed to adsorb at the interface 0.5 h before the injection of BSA (t = 0 h). DPPC is injected 90 min later.

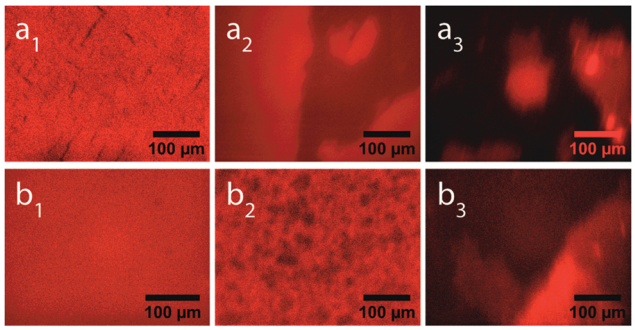

Fig. 4 Fluorescence micrographs of the sequential adsorption of BSA and DPPC (injected 1.5 h after BSA) at the air/buffer interface (a) in the presence and (b) absence of *F*-hexane. Adsorption in the presence of *F*-hexane after 2.3 h (a_1), 3.3 h (a_2), and 7.5 h, and in absence of the fluorocarbon gas after 3.2 h (b_1), 3.8 h (b_2) and 8.2 h (b_3). The concentrations were DPPC (3×10^{-3} mol L^{-1}; BSA: 7.5×10^{-7} mol L^{-1}).

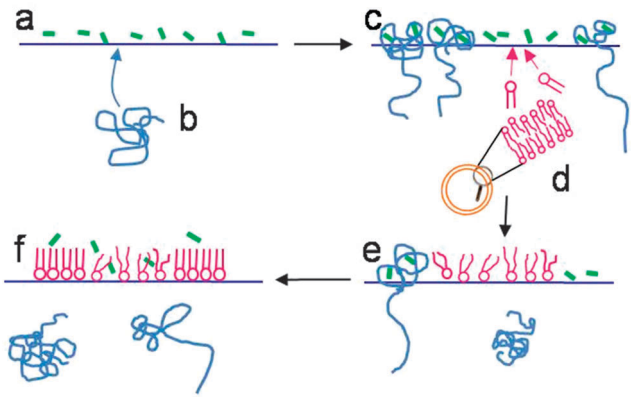

Scheme 2 (a) *F*-hexane (green) quickly adsorbs at the interface and (b) BSA (blue) adsorbs from the solution. (c) *F*-Hexane induces the unfolding of BSA and (d) facilitates recruitment of DPPC (magenta) at the interface where it forms a dilute phase (e). (f) The DPPC dilute-to-condensed phase transition occurs; the unfolded BSA molecules are displaced from the interface after the transition.

are seen to grow in number and size over time forming large plates (Fig. $4a_2$) that progressively nearly cover the whole water surface (Fig. $4a_3$). On the other hand, in the absence of *F*-hexane, the micrographs remain uniformly bright (similar to those obtained when BSA is adsorbed alone) for a longer time (Fig. $4b_1$). It is only after ~3.8 h (2.2 h after DPPC injection) that the dark structures begin to appear (Fig. $4b_2$), slowly growing in size and number to form plates after ~8 h only (Fig. $4b_3$).

We picture the sequential adsorption of the competing compounds as shown in Scheme 2. The fluorocarbon adsorbs first, and very rapidly, at the interface (Scheme 2a). Once there, it interacts with the BSA molecules that are reaching the interface (Scheme 2b). The fluorocarbon is likely hosted in the hydrophobic cavities of BSA located in sub-domains IIA and IIIA (Scheme 2c), and promotes the unfolding of the protein at the interface, with its hydrophilic sequences stretched in water and its hydrophobic sequences bundled at the surface. This appears to be reasonable since fluorinated anesthetics and perfluoroalkylated amphiphiles have indeed been shown to bind with BSA in solution.[20,21]

The unfolded conformation of BSA and the presence of free *F*-hexane, which breaks the interfacial structure of water, result in an acceleration of the adsorption of DPPC at the interface (Scheme 2d). DPPC first forms a dilute phase (Scheme 2e). When the density of the latter becomes large enough to induce the dilute-to-condensed transition, the remaining BSA molecules are ejected (Scheme 2f). The fact that the protein is unfolded, rather than in a globular conformation, facilitates its ejection toward the aqueous phase.

In summary, we show that a fluorocarbon gas acts as an efficient promoter of protein displacement at the air/water interface of a bubble submitted to sinusoidal oscillations. This is expected to provide an efficient tool for the design and evaluation of lung surfactant substitutes. More generally, this novel property of the biologically inert fluorocarbons can be added to the toolbox of biomolecular sciences, particularly in the investigation of dynamic and transport properties in systems for which reaching equilibrium is too slow under standard experimental conditions.[14,22]

The authors thank the European Community's Seventh Framework Program (FP7 2007–2013; grant no NMP3-SL-2008-214032). They acknowledge the French National Research Agency (ANR, grant no 2010-BLAN-0816-01) and the GIS Fluor for financial support, and Mariana Sontag González for her contributions to Langmuir trough experiments. M.V. is grateful to the graduate college program GRK 1114 supported by the German Science Foundation. M.T. is a member of the German Excellence Cluster "Cell Network" and the Helmholtz Program "BioInterfaces"

Notes and references

1 R. H. Notter, *Lung surfactants: Basic Science and Clinical Applications*, Marcel Dekker, New York, 2000.
2 B. A. Holm, G. Enhorning and R. H. Notter, *Chem. Phys. Lipids*, 1988, **49**, 49–55.
3 J. A. Zasadzinski, P. C. Stenger, I. Shieh and P. Dhar, *Biochim. Biophys. Acta, Biomembr.*, 2010, **1798**, 801–828.
4 Y. Y. Zuo, R. A. W. Veldhuizen, A. W. Neumann, N. O. Petersen and F. Possmayer, *Biochim. Biophys. Acta*, 2008, **1778**, 1947–1977.
5 J. A. Zasadzinski, J. Ding, H. E. Warriner, F. Bringezu and A. J. Waring, *Curr. Opin. Colloid Interface Sci.*, 2001, **6**, 506–513.
6 X. Wen and E. I. Franses, *Colloids Surf., A*, 2001, **190**, 319–332.
7 P. N. Nguyen, G. Waton, T. Vandamme and M. P. Krafft, *Soft Matter*, 2013, **9**, 9972–9976.
8 P. N. Nguyen, G. Waton, T. Vandamme and M. P. Krafft, *Angew. Chem., Int. Ed.*, 2013, **52**, 6404–6408.
9 D. J. L. McIver, F. Possmayer and S. Schurch, *Biochim. Biophys. Acta*, 1983, **751**, 74–80.
10 F. Gerber, M. P. Krafft, T. F. Vandamme, M. Goldmann and P. Fontaine, *Angew. Chem., Int. Ed.*, 2005, **44**, 2749–2752.
11 F. Gerber, M. P. Krafft, T. F. Vandamme, M. Goldmann and P. Fontaine, *Biophys. J.*, 2006, **90**, 3184–3192.
12 H.-J. Lehmler, *Expert Opin. Drug Delivery*, 2007, **4**, 247–262.
13 M. P. Krafft, *Biochimie*, 2012, **94**, 11–25.
14 J. G. Riess, *Chem. Rev.*, 2001, **101**, 2797–2920.
15 E. S. Schutt, D. H. Klein, R. M. Mattrey and J. G. Riess, *Angew. Chem., Int. Ed.*, 2003, **42**, 3218–3235.
16 J. R. Lindner, *Nat. Rev. Drug Discovery*, 2004, **3**, 527–532.
17 J. G. Riess, *Curr. Opin. Colloid Interface Sci.*, 2009, **14**, 294–304.
18 D. E. Graham and M. C. Phillips, *J. Colloid Interface Sci.*, 1979, **70**, 403–414.
19 B. A. Noskov, A. A. Mikhailovskaya, S.-Y. Lin, G. Loglio and R. Miller, *Langmuir*, 2010, **26**, 17225–17231.
20 R. G. Eckenhoff and J. W. Tanner, *Biophys. J.*, 1998, **75**, 477–483.
21 P. D. Jones, W. Hu, W. de Coen, J. L. Newsted and J. P. Giesy, *Environ. Toxicol. Chem.*, 2003, **22**, 2639–2649.
22 M. Cametti, B. Crousse, P. Metrangolo, R. Milani and G. Resnati, *Chem. Soc. Rev.*, 2012, **41**, 31–42.